# Evaluation of high-voltage circuit breaker performance with a validated arc model

# Evaluation of high-voltage circuit breaker performance with a validated arc model

R.P.P.Smeets and V.Kertész

**Abstract:** A digital current-zero measuring system was used to monitor about 200 zero crossings of short-line fault currents in three designs of commercial high-voltage circuit breakers. The breakers were subjected to standard IEC 60056 tests in a high-power laboratory. With these results, an empirical arc model was derived, based on the series connection of three classical modified Mayr models. It was found that only three 'free' parameters, extracted from the arc voltage and current during the prezero period can describe the state of the breaker after each test. With this model, the margin of the interrupting capability could be directly obtained. A strong relation between this margin and the arc conductivity at current zero can be established. Independent of arcing time, arcing current and state of the breaker, it was found that the current zero conductivity must decrease to 1–2ms (only depending on the design of the breaker) to make a successful interruption possible.

## 1 Introduction

High-voltage circuit breakers (CBs) have a vital function in isolating faulted sections of power networks. At short-circuit current zero (CZ), the instantaneous energy input into the arc is minimal, enabling the arc to extinguish. Immediately after the extinction of the arc, the power network reacts with a transient recovery voltage (TRV) that stresses the gap.

The ability of the CB to interrupt is verified in high-power laboratories. Although the main aim of high-power tests is to prove the ability of a CB to perform a given switching duty, information on the 'quality' of that performance is usually not available. An international research program was set up by KEMA and sponsored by the European Commission, aimed at extracting the maximum possible amount of information on the interruption process during high-power tests. This information is presented and performance margins of three different CBs are investigated.

## 2 Measuring system

A new measuring system of high accuracy and high resolution was developed, based on KEMA's long experience [1]. With the aid of an 'intelligent' triggering module, with this system, current and voltage during up to four consecutive CZs having a total window of 6.4ms are automatically recorded with a sampling frequency of 40MHz combined with a 12 bit resolution. A specially designed wideband (> 10MHz) Rogowski coil is used as a current sensor; the arc voltage is measured with wideband (> 5MHz) voltage dividers. With custom-made signal processing software, a flexible visualisation of arc current, voltage, conductivity, etc. is possible [2]. The digitising part of the system, placed on floating potential in the close vicinity of the test object, stores the data locally. Immediately after the test, data is sent through an optical fibre to the control centre. Current levels down to 50mA could be measured.

## 3 Measurements

A program of high-power tests set up a database of CZ information of a number of commercially available modern high-voltage $SF_6$ CBs of various technology (puffer-type, double nozzle type and selfblast type). Tests were performed under 90% short-line fault (SLF) conditions (IEC 60056) at 60Hz. In Table 1, an overview is given of the number of tests, number of current zeros for each CB, and the number of resultant interruptions (Int.) and reignitions (Reign.). All breakers were in new condition before the tests.

**Table 1: Overview of tests**

| Rating of CB | Short | Circuit | Tests | $CZ_s$ | Int. | Reign. |
|---|---|---|---|---|---|---|
| 72.5kV @ 31.5kA | CB72 | direct | 28 | 64 | 24 | 40 |
| 123kV @ 31.5kA | CB123 | synthetic | 33 | 33 | 24 | 9 |
| 145kV @ 31.5kA | CB145 | direct | 27 | 50 | 26 | 24 |
| 145kV @ 31.5kA | CB145 | synthetic | 27 | 27 | 21 | 6 |

An example of a test result is the arc current and voltage during three consecutive CZs in one test shown in Fig. 1. Two reignitions labelled 1 and 2 (after arcing times of 7.9 and 16.3ms) and one interruption labelled 3 (after 24.6ms) are shown. In this example, a postarc current of several amps distorted the TRV heavily. CBs in a good condition normally produce postarc currents below 100mA or so. In the event of unusually large values of postarc current (as in Fig. 1) it was the experience that the breaker chamber is very near to the end of its ability to clear the SLF.



*IEE Proceedings* online no. 20000238

*DOI*: 10.1049/ip-gtd:20000238

Paper first received 6th July and in revised form 30 November 1999

The authors are with KEMA High-Power Laboratory, Utrechtseweg 310, 6812 AR Arnhem, the Netherlands

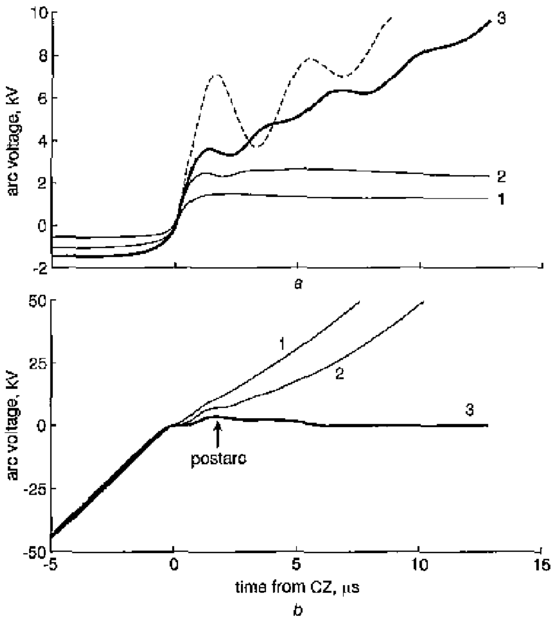


**Fig. 1** *Wavetraces of arc current and arc voltage of three consecutive (1, 2, 3) arcing current zeros in one breaking operation of CB72*
*a* Arc voltage showing normal TRV resulting from interruption with very small (< 50mA) postarc current
---- 'Normal' TRV; ▬▬ TRV
*b* Arc current

## 4 New arc model

### 4.1 Model philosophy

The new model is founded on classical results. A great deal of work on arc modelling was carried out by CIGRE WG 13.01, resulting in the publication of a number of surveys of the state of the art [3–5].

Considering the very different time scales of the physical processes in the chamber, the modelling concept is based on the division of the whole interruption process into a period where 'slow' and a period where 'fast' phenomena prevail. In the slow period the arc-circuit interaction is essentially weak, and the current is imposed by the circuit. The fast period starts at some tens of μs before CZ. In the slow period (starting at the contact separation) the physical conditions (pressure build up, arc temperature, etc.) are set that determine the initial conditions for the fast period. The characteristic time constants of the slow processes are probably some hundreds of μs or more, and for the fast processes some μs or less. A sophisticated slow model must contain a large number of parameters depending on the chamber design and internal condition, the gas pressure, and the stress factors like current history and arcing time. It is most likely that the slow model is strongly CB dependent.

It can be assumed that the fast processes are determined by the evolution of the relevant quantities during the slow period and the properties of the $SF_6$ gas. Consequently, the fast model is probably only weakly dependent on the CB, and is determined mainly by the $SF_6$ properties. Its parameters should reflect the initial conditions determined by the slow period. In this sense, although only a tiny portion of the entire arcing time is taken into account during the fast period model, the whole arcing history has a fundamental impact on the phenomena in the fast period.

Based on this philosophy, the fast model can be used in its own right, completely separated from the slow model, provided the parameters reflecting the initial conditions are known. Because of the extreme rapidity of processes in $SF_6$ gas, presumably only energy exchange takes place during the fast period. Flow and other complex 3D processes are not likely to play an essential role. Therefore a lumped model could suffice, accomplished by a set of ordinary differential equations (ODEs) [6]. Arc-circuit interaction is obviously strong and the time constants are very small. Consequently, in the arc-circuit interaction only those factors play a role that are related to fast changes, like parasitic elements close to the breaker, the rate of rise of the current close to CZ, and the initial rate of rise of the TRV.

In our opinion higher-order ODE modelling is necessary because the fast period itself has quite different time scales owing to varying conditions along the arc channel.

### 4.2 Outline of new model

Making extensive use of the new CZ data base, it was possible to derive a new (fast) black-box model, based on a combination of the classical proven approaches by Mayr [7] and Cassie [8]. The parameters of this model have been extracted from experimental data creating the 'engineering' part of the model.

The new model consists of three modified Mayr models connected in series representing three series arc sections each with three parameters: the time constant $T_i$ [s], the quantity $\Pi_i$ [$A^{\lambda-1}V^{3-\lambda}$] related to power loss and the dimensionless model parameter $\lambda_i$ ($i$ index for each submodel)

$$\frac{dG_i}{dt} = \frac{1}{\Pi_i T_i} G_i^{\lambda_i} U_i^2 - \frac{1}{T_i} G_i \qquad i = 1, 2 \text{ and } 3 \quad (1)$$

where $G_i$ [S] is the conductivity, $U_i$ [V] the arc voltage and $t$ [s] is the time. If $\lambda = 2$ eqn. 1 reduces to the classical Mayr model [7] with $\Pi = P_0$ [W] the usual power loss constant. If $\lambda = 1$ eqn. 1 is the Cassie model [8] and $\Pi = U_o^2$, with $U_o$ [V] is the classical steady-state arc voltage.

The following equations describe the directly measurable current I and voltage U and the conductivity G:

$$\frac{1}{G} = \sum_{i=1}^{3} \frac{1}{G_i} \qquad U = \sum_{i=1}^{3} U_i \qquad I = UG \qquad (2)$$

This model contains nine parameters in principle, however, six of them proved to be empirical constants having the following values and relationships:

$$\lambda_1 = 1.4; \quad \lambda_2 = 1.9; \quad \lambda_3 = 2.0$$
$$T_2 = T_1/k_1$$
$$T_3 = T_2/k_2$$
$$\Pi_3 = k_3 \Pi_2$$

Based on the measuring results, the first submodel was chosen to be a Mayr–Cassie type arc, the second one almost a pure Mayr type arc, and the third one is a pure Mayr arc. The values of $\lambda_i$ remain the same throughout all the tests. The breaker parameters $k_1$, $k_2$ and $k_3$ depend on the actual CB design, and keep their validity during all tests on one breaker, see Table 2. $T_1$, $\Pi_1$, and $\Pi_2$ are considered then to

**Table 2: Breaker parameters**

| | | | | |
|---|---|---|---|---|
| Model parameters (constant in all tests) | $\lambda_1, \lambda_2, \lambda_3$ | | | |
| circuit breaker parameters (vary from CB to CB) | | $k_1$ | $k_2$ | $k_3$ |
| | CB72 | 5.7 | 5 | 100 |
| | CB123 | 4.9 | 5 | 100 |
| | CB145 | 5.7 | 10 | 100 |
| State parameters (vary from test to test) | $T_1, \Pi_1, \Pi_2$ | | | |

be the 'free' parameters, describing the state of the CB during each interruption attempt. These parameters have a large range, and depend on the actual test conditions (mainly arcing time, slope of arc current *di/dt* denoted by $S$) and the state of degradation of the CB. Nevertheless, clear differences can be seen reflecting the different CB designs. In Fig. 2, the cumulative distribution of the measured values of the time constant $T_3$ and the cooling power constant $P_0 = \Pi_3$ of the third (pure Mayr) series arc have been visualised.

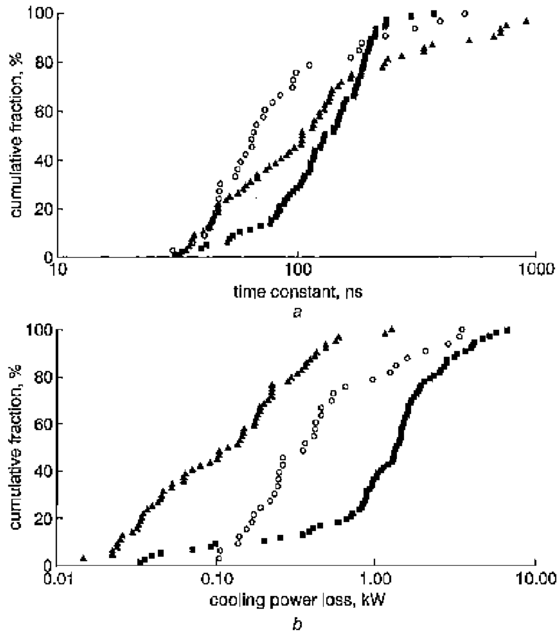


**Fig. 2** *Cumulative fractions of state parameters of third series arc in new model*
*a* Time constant $T_3$
*b* Cooling power loss $\Pi_3$ ($\Pi_3 = P_0$)
▲ CB72
○ CB123
■ CB145

### 4.3 Model validation

The main idea is to make distinction between the stochastic and the deterministic part of the interruption process. The actual shape of the arc channel in the critical time interval (several μs) before CZ is a result of a stochastic process. However, once a specific channel has been developed, it is very likely that the interruption process from that point is essentially deterministic. Therefore the actual measured traces of each CZ are taken to extract arc parameters that are exclusively related to that specific case. Due to the fact that the very small value of postarc current of 'healthy breakers' cannot be measured accurately, only arc information up to and including CZ is used. From the prezero region, the arc parameters of each individual test were extracted using a special multidimensional successive gradient method.

Next, with these arc parameters, the model of eqn. 1 with eqn. 2 was used to calculate the maximum value of power frequency current slope $S_L$ that the arc would interrupt. Then this value is compared to the actual $S$ during the test. Thus if $S_L < S$ the model predicts a reignition, if $S_L > S$ an interruption is predicted. This prediction is ultimately confronted with the real measured result of the interruption attempt after some optimisation stages resulting in an overall model performance of 91% of the interruption attempts, the result of which is predicted correctly. Fig. 3 illustrates the course of the described validation procedure.

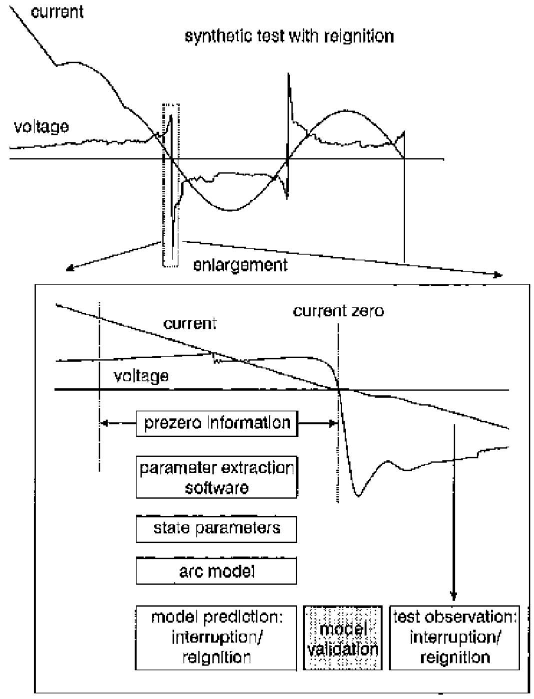


**Fig. 3** *Illustration of validation method, here with synthetic test including interruption failure of CB123*

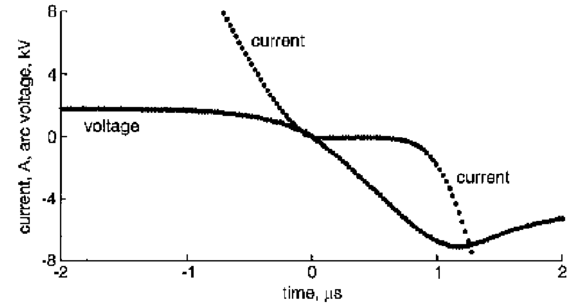


**Fig. 4** *Example of arc current and voltage wavetraces near current zero in mixed type of reignition in CB123*
Dots indicate sample points

In some cases, where prediction is 'interruption' and observation is 'failure', a so-called 'mixed' type of failure was observed (Fig. 4). The part of the arc channel that is described by the third (purely Mayr) equation of eqn. 1 having the smallest time constant is mainly responsible for the interruption and the (immediate) thermal reignition. Because of this small time constant (30–200ns), this section of the arc cools down much faster than the other parts. It seems that the failure is a dielectric reignition from the point of view of the Mayr arc part, and a thermal failure if the remainder and still hot parts of the arc are considered.

Another check of the validity of the present model is its ability to simulate the correct wave traces. It was observed that from several hundreds of μs before CZ up to CZ the fitting is very good. The model is correct also in predicting small post arc currents in accordance with the measurements. A typical example of the correct wave trace simulation is shown in Fig. 5 (Figs. 5*a* and *b* show the same CZ with different time scale).

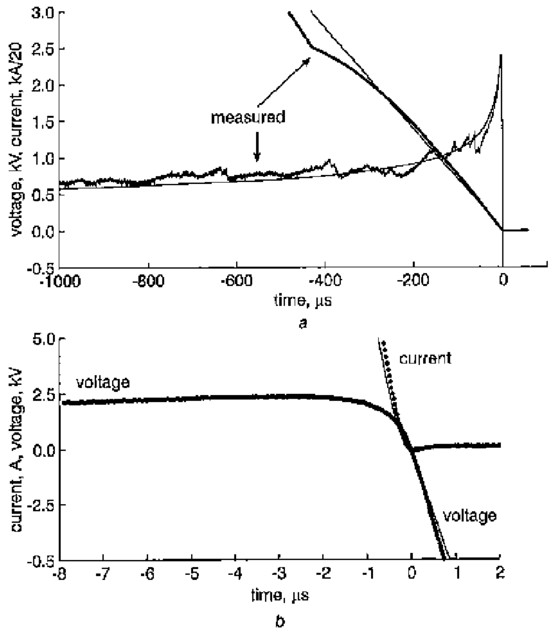


**Fig. 5** *Comparison of measured and calculated current and voltage wave-traces (CB123)*
(*a*) 1ms time-scale
(*b*) 10µs time-scale
——— simulated waveshapes
......... measured signals

## 5 Interruption performance evaluation

Since the new model can theoretically predict the maximum possible *di/dt* ($S_L$) the arc is able to interrupt at the specific circuit conditions and at the specific state of the CB chamber, the margin of interruption can be estimated when this quantity is compared to the actual *di/dt* ($S$). A suitable parameter to quantify this margin is

$$M = \frac{S_L - S}{S_L + S} \tag{3}$$

The value of $M$ is between −1 and 1. Negative $M$ indicates reignition, positive value implies interruption. With the quantity $M$, it is possible to map the degradation of the breaker during the succession of test. An example (CB72) is given in Fig. 6. Three poles (A, B and C) of the same CB were tested using the same circuit.

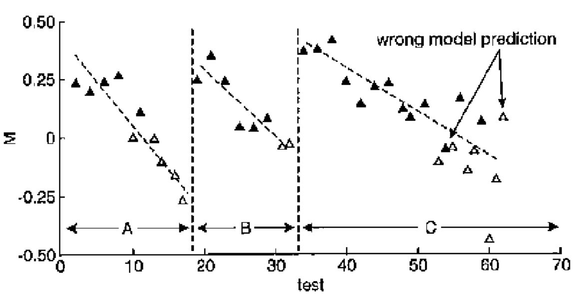


**Fig. 6** *Interruption margin M of circuit breaker CB72 for each pole during the succession of SLF tests*
A tested with 24.4 $kA_{RMS}$; B tested with 22.1 $kA_{RMS}$; C tested with 17.4 $kA_{RMS}$)
△ observed reignitions
▲ observed interruptions

The following observations from Fig. 6 must be emphasised:

(a) There is a clear net decrease of margin during the progress of tests on every pole, reflecting the degradation of the breaker by the tests.

(b) In all but two cases (indicated with 'wrong model prediction') the new model predicts from its prezero input successfully an interruption or reignition

(c) The rate of degradation is clearly depending on the amount of power-frequency current stress (pole A 24.4, pole B 22.1, pole C 17.4 $kA_{RMS}$).

From these observations, the concept of interpreting the margin quantity $M$ as a valid measure of CB degradation is clear.

As another example, the margin quantities of the interruption attempts plotted in Fig. 1 are given: Attempt 1: $M = -0.17$, attempt 2: $M = -0.083$ and attempt 3 (interruption) $M = 0.015$. The latter (very small margin) represents the deteriorated state of the chamber only marginally being able to clear the fault. In Fig. 7, the margin quantity for each interruption attempt is plotted against the arcing time. A steady increase of $M$ can be noted up to the minimum arcing time (around 8ms), followed by an optimum near 12ms, showing the breaker's best performance.

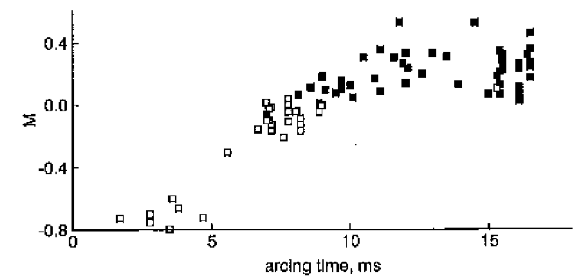


**Fig. 7** *Margin M of interruption plotted against arcing time for CB145*
□ observed reignitions
■ observed interruptions

A good candidate of a physical parameter that is indicative for the actual ability of the breaker to clear the SLF is the conductivity of the breaker at CZ ($G_0$). In Fig. 8, the relationship between this residual conductivity is plotted against the margin $M$ for the breakers under test, thus establishing a direct link between $G_0$ and the 'quality of the interruption'. The dependence of $G_0$ is only marginally on the stress factors. As a general rule, however, it can be concluded from the actual measurements that interruption becomes possible when arc conductivity has dropped below about 1–2mS (see Fig. 9, the enlargement around the interruption limit $-0.05 < M < 0.05$ of Fig. 8).

## 6 Summary and conclusions

A new empirical arc model has been presented that has been shown to predict correct results of standard (IEC 60056) SLF interruption tests based on prezero information. Arc voltage and arc current wave traces were recorded with a tailor-made high-frequency high-resolution current-zero data-aquisition system. Data from approximately 180 tests were used for the parameter definition and evaluation of the new model, a series connection of three modified Mayr equations, yielding only three free 'state' parameters (varying from test to test).

With the aid of the model, margins of individual interruptions can be specified. Its application to commercially available power CBs of various technologies and rating (≤ 145kV) has shown that the process of CB degradation can be mapped by the present method. Further, it was made plausible that the arc conductivity at CZ (relatively

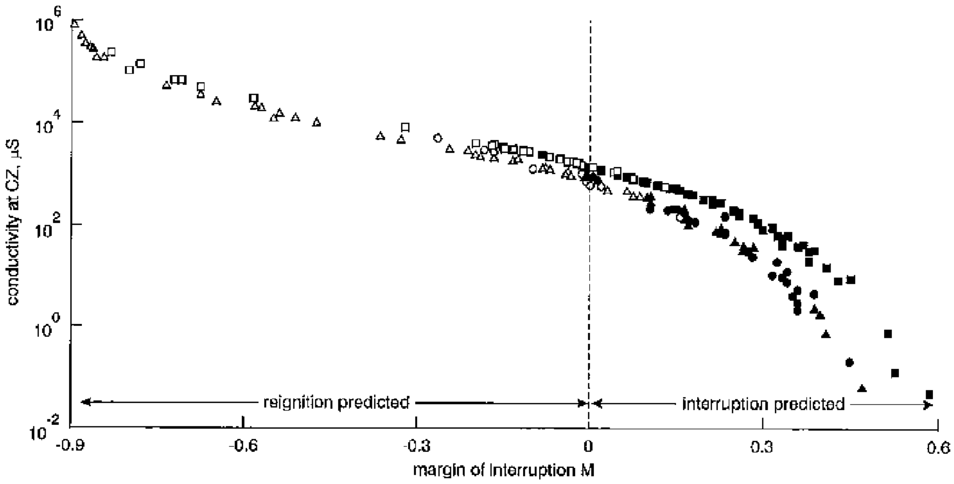


**Fig.8** *Correlation between current-zero conductivity and interruption margin M for all breakers with enlargement around area of critical interruption*
▲ CB72
● CB123
■ CB145

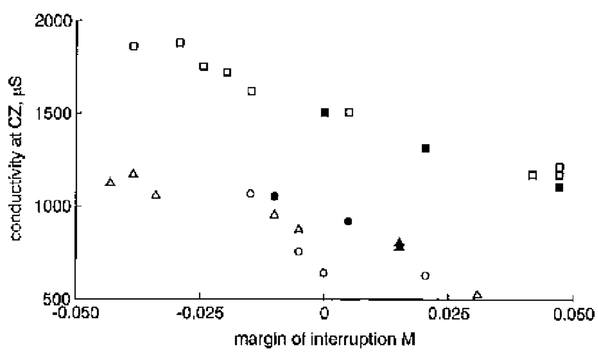


**Fig.9** *Enlargement around interruption limit shown in Fig. 8*
▲ CB72
● CB123
■ CB145

easy accessible for measurement) is a reasonable indicator for the margin of the interruption. Knowledge of the margin can be applied in the following fields:

- development of CBs by manufacturing companies
- application of CBs in non-standard circuits and for non-standard ratings
- estimation of the state of a breaker after extended service
- development of future standards
- dedicated high-power testing and comparison of test-circuits

Given the wide range of the arc parameters describing the actual state of the CB, it is our opinion that a generally applicable arc model such as often offered in network analysis software does not exist, not even for a single CB design.

## 7 Acknowledgment

Thanks are due to Dr. H. Knobloch (Siemens AG) and to Dr. C. Neumann (RWE Energie AG) for supplying some of the test objects. Thanks are also due to Mr. A. Even (Laborelec cv.) and Dr. P. Scarpa (Liège University) for the opportunity to do various types of experiments in their laboratories and to Prof. L. van der Sluis (Delft University) for discussion.

## 8 References

1 DAMSTRA, G.C., and KERTÉSZ, V.: 'Development and application of a 10 MHz digital system for current-zero measurements', *IEE Proc.-Sci. Meas. Technol.*, 1995, **142**, (2), pp. 125–132

2 SMEETS, R.P.P., EENINK, A.H., and KERTÉSZ, V.: 'A new high-resolution high-frequency current-zero measuring system'. Presented at the ERA conference on *Measurement and calibration in high-voltage testing*, 1998, Paper 1.2

3 CIGRE WORKING GROUP 13.01, : 'Practical application of arc physics in circuit breaker. Survey of calculation methods and application guide', *Electra*, May 1988, **118**, pp. 66–79

4 CIGRE WORKING GROUP 13.01, : 'Applications of black box modelling to circuit breakers', *Electra*, August 1994, **149**, pp. 41–71

5 CIGRE WORKING GROUP 13.01, : 'Survey on analytical and graphical tools for circuit breaker behaviour description'

6 HABEDANK, U.: 'Application of a new arc model for the evaluation of short-circuit breaking tests', *IEEE Trans.*, 1993, **PWRD-8**, (4), pp. 1921–1925

7 MAYR, O.: 'Beiträge zur Theorie des Lichtbogens und seiner Löschung', *Archiv für Elektrotechnik*, 1943, pp. 588–608

8 CASSIE, A.M.: 'Arc rupture and circuit severity: a new theory'.CIGRE report, 1939